

Electron Microscopy I

Lecture 11

TT.Prof. Dr. Yolita M. Eggeler

Laboratory for electron microscopy,
CFN building, 2nd floor, room 215

yolita.eggeler@kit.edu

Phone 608-43724

Electron microscopy I

1. From light microscopy to electron microscopy
2. Practical aspects of transmission electron microscopy (TEM) and scanning transmission electron microscopy (STEM)
3. Electron diffraction in the solid state/kinematic diffraction theory
4. Contrast formation and practical examples of the illustration of crystalline objects in solid state and materials research
5. Dynamic electron diffraction
6. Imaging of the crystal lattice/high-resolution electron microscopy (HRTEM)
 - 6.1 Introduction and practical aspects of HRTEM
 - 6.2 Dynamic electron diffraction in the HRTEM
 - 6.3 Image formation in the HRTEM
7. Electron holography

6.1 Introduction and practical aspects of high-resolution transmission electron microscopy (HRTEM)

Prerequisite for high-resolution imaging of the crystal lattice

- **Coherent interference** of electron waves



- Incident electron wave with high spatial and temporal coherence

- *extremely thin samples, as inelastic scattering processes become more dominant with increasing sample thickness and destroy the coherence of the electrons*

in practice: maximum sample thicknesses of around 50 nm for materials with low density and low atomic number such as Si or Al (maximum thickness depends on atomic number/material density and electron energy)

- **Most important imaging parameters:** **Sample thickness t** and **objective lens defocus Δf**
- **Dynamic electron diffraction in zone-axis orientation even with very small sample thicknesses $\approx > 5$ nm**, as Bragg diffraction occurs in several reflexes and not just in one reflex as with the two-beam condition



Strong thickness dependence of the wave function on the underside of the sample

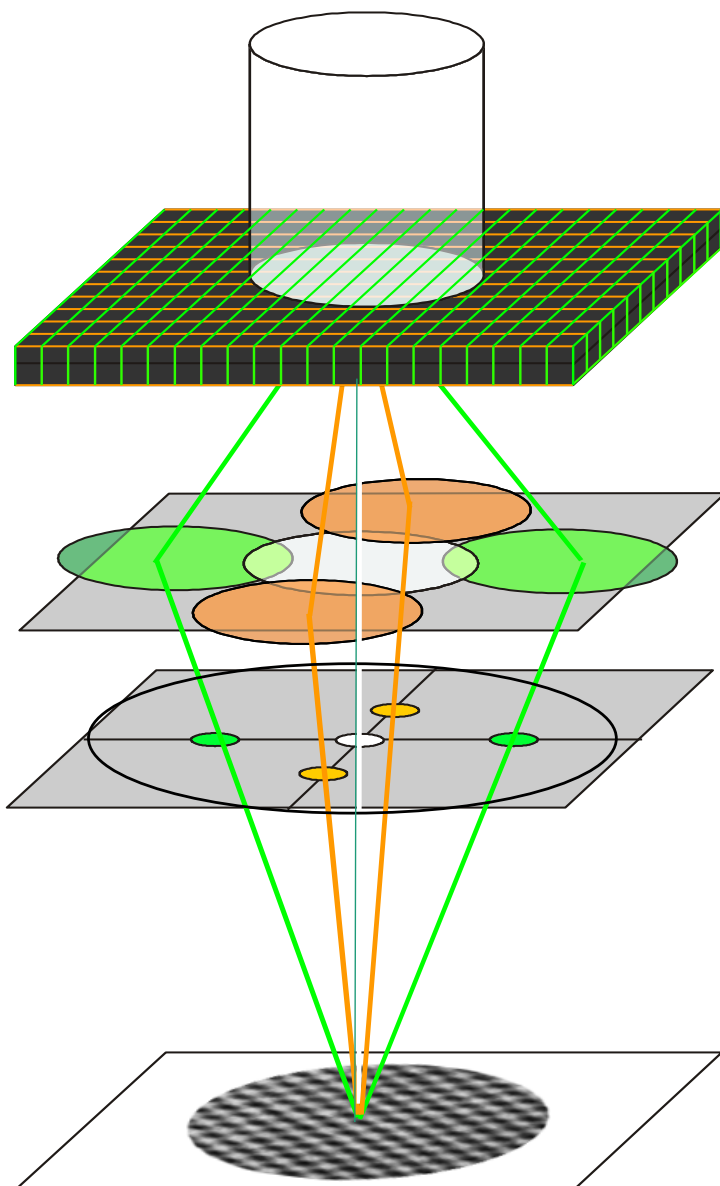
Complex wave function that does not necessarily reflect the projected crystal potential

- **Modification of the wave function by imaging in the microscope due to the effects of lens aberrations**



Image simulations necessary for understanding HRTEM images

6.1 Introduction and practical aspects of high-resolution transmission electron microscopy (HRTEM)

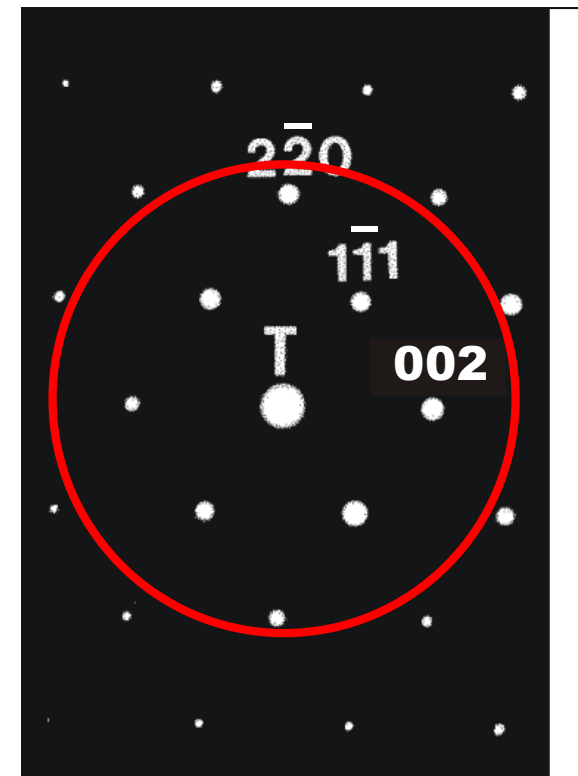


Sample in zone-axis orientation

Objective lens

Diffraction image lens aperture with large diameter

Image wave function: *Coherent* interference from Bragg-diffracted waves

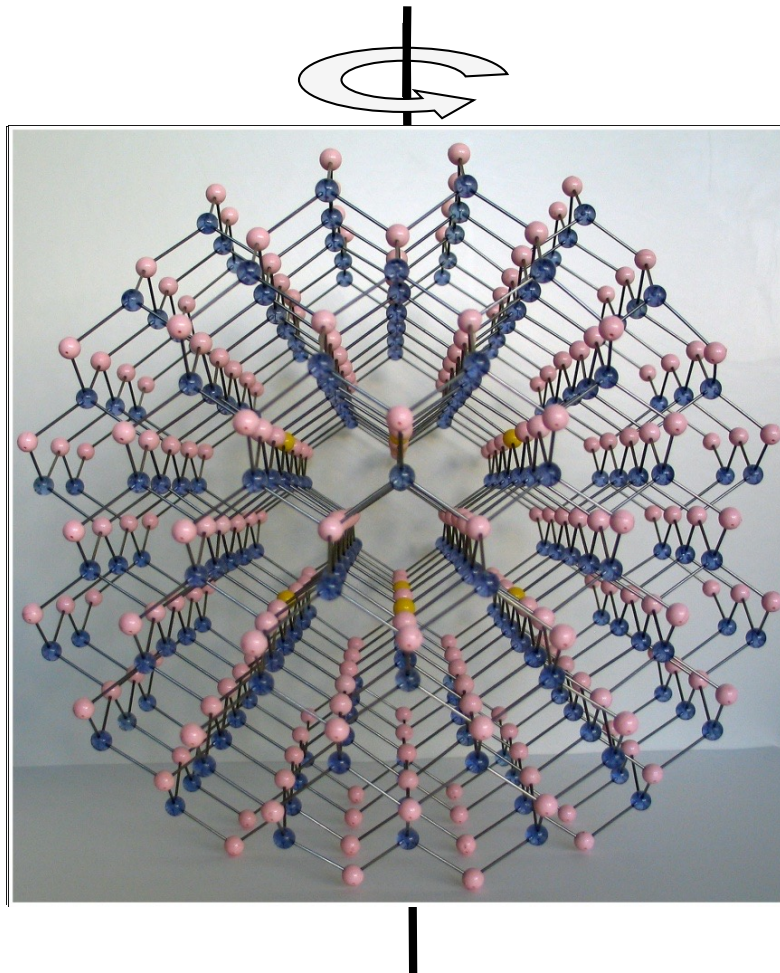


Diffraction image GaAs in [110] zone axis

Large lens aperture
→ Selection of several reflexes for mapping

6.1 Introduction and practical aspects of high-resolution transmission electron microscopy (HRTEM)

Resolution of atomic columns: Spacing of the atomic columns > Resolving power



- Distances between the atomic columns are larger for crystal orientations along low-index crystal directions (zone axes), e.g. directions of type [100], [110], [111] and [112]
- With highly indexed directions, the distances between the atomic columns are usually too small

Orientation of the sample along low-indexed zone axis

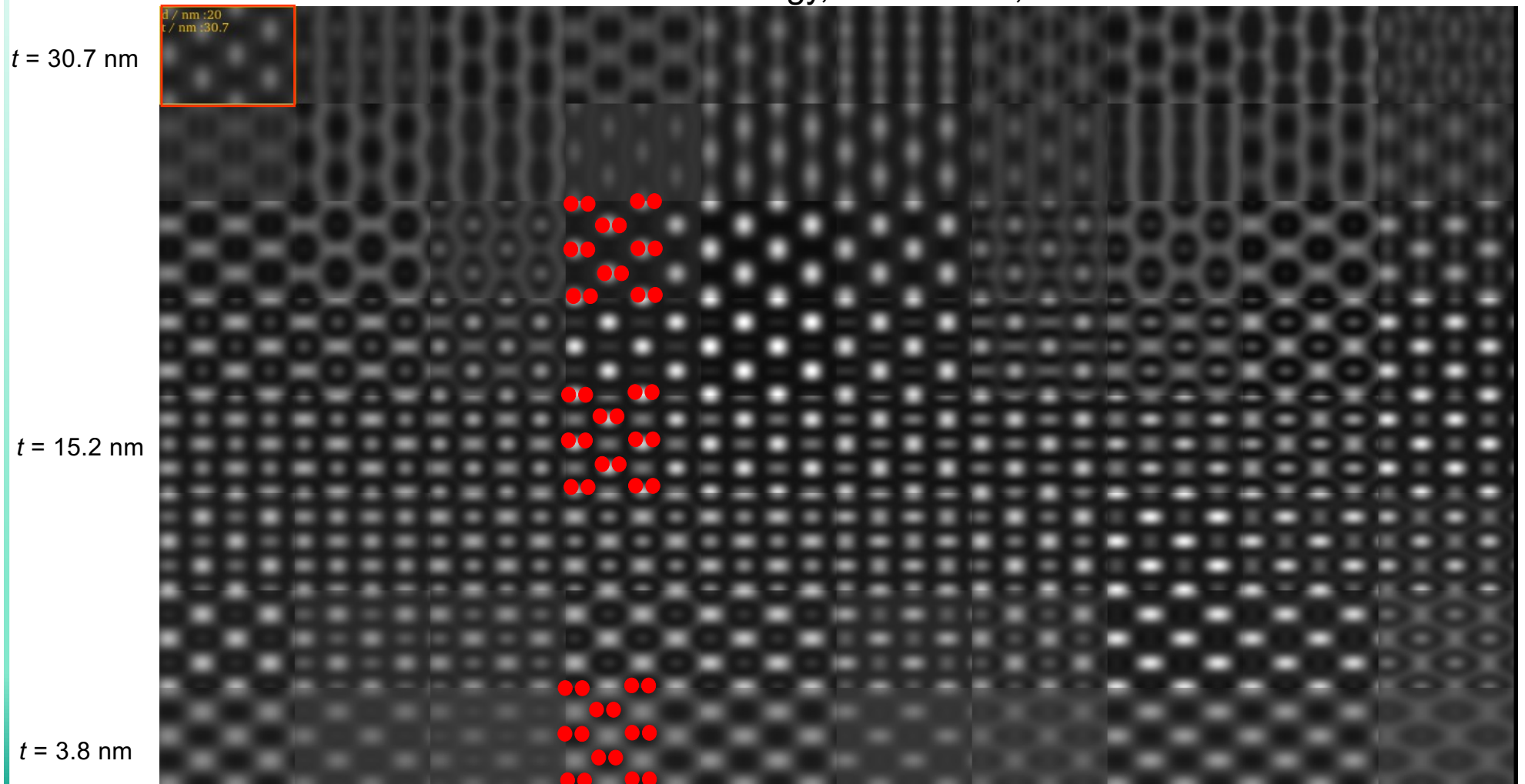
6.2 Dynamic electron diffraction in the HRTEM

Image simulations for silicon in [110] zone axis: dependence of the image pattern on the sample thickness t and the defocus of the objective lens Df

$\Delta f = -20$ nm

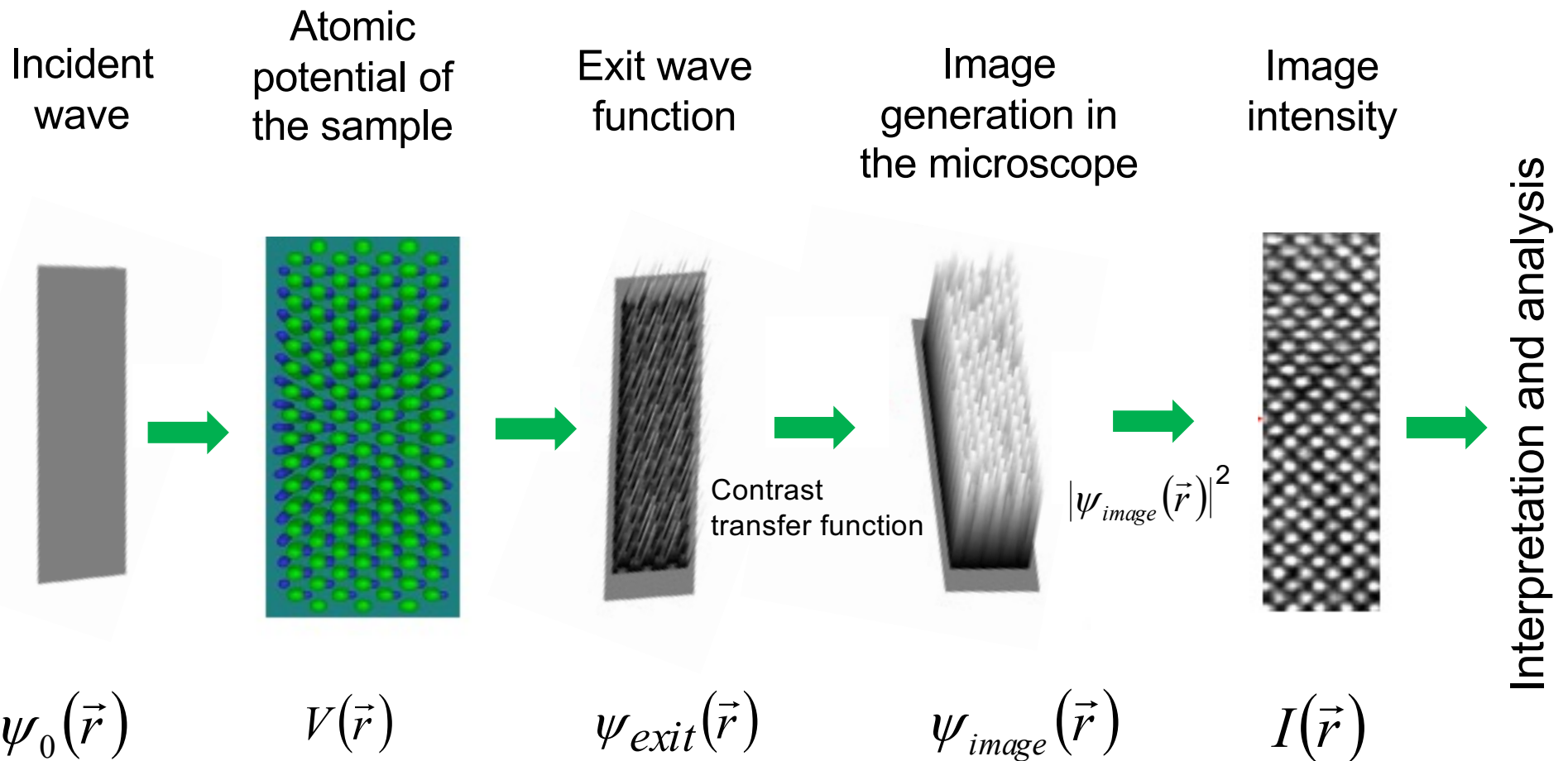
200 keV electron energy, Cs=1.2 mm, Cc=1.2 mm

$\Delta f = -120$ nm



6.2 Dynamic electron diffraction in the HRTEM

Image formation in the HRTEM



6.2 Dynamic electron diffraction in the HRTEM

Different methods for calculating the exit wave function taking into account multiple scattering processes

- two methods:
 - *Bloch wave method*
 - *Multislice method* for structures with a large number of atoms

Solution of the Schrödinger equation (Bloch wave method)

Extension to multi-beam case (only two-beam case considered in chapter 5)

- ***symmetrical Laue case*** (zone axis orientation) - consideration of more than two reflexes and thus also more than two Bloch waves to describe the wave function
time-independent Schrödinger equation

$$-\frac{\hbar^2}{8\pi^2 m} \nabla^2 \psi(\vec{r}) - eV(\vec{r})\psi(\vec{r}) = eU\psi(\vec{r})$$

- Total wave function as the sum of all N excited Bloch waves

$$\psi = \sum_{j=1}^N \alpha^j b^j(\vec{k}^j, \vec{r})$$

α^j : excitation coefficients depend on boundary conditions, e.g. sample thickness and excitation error of Bragg reflexes


6.2 Dynamic electron diffraction in the HRTEM

- Further procedure analogous to the two-beam case → Inserting the approaches for the periodic potential and Bloch waves (taking into account excitation errors of the Bragg reflexes) into the Schrödinger equation


$$V(\vec{r}) = \sum_{\vec{g}} V_{\vec{g}} \exp(2\pi i \vec{g} \vec{r})$$
$$b^j(\vec{k}^j, \vec{r}) = \sum_{\vec{g}} C_{\vec{g}}^j \exp(2\pi i (\vec{k}^j + \vec{g} + \vec{s}) \vec{r})$$

instead of a system of equations with two equations for only two \vec{g} -vectors (cf. Eq. (13) in chapter 5) **an equation for each relevant mapping vector \vec{g}**

- Solution of the system of equations (eigenvalue problem) to determine the Bloch wave coefficients and wave number vectors

 Result: Coefficients $C_{\vec{g}}^j$ and the wave number vectors \vec{k}^j of the Bloch waves and thus also the total wave function $\psi(\vec{r})$


(The number of Bloch waves for a reasonable description of the wave function depends on the size of the unit cell, its symmetry and the number of atoms and atomic species as well as the zone axis orientation of the sample)

- For the simulation of defect structures with a large number of atoms: high computing time expenditure  Supercomputer required

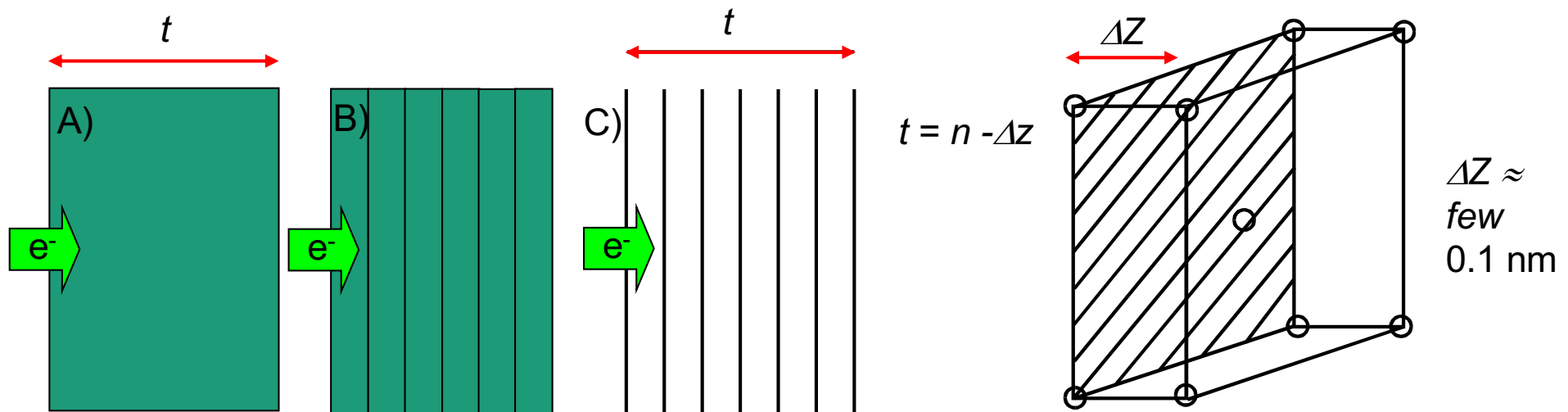
6.2 Dynamic electron diffraction in the HRTEM

Multislice process

- Alternative method for solving the Schrödinger equation for complex crystal structures with many and/or different atoms and for defect structures

 Development of a numerical iteration method for calculating the wave function (Cowley and Moody)

- **Multislice = multi-slice process:**
Decomposition of the interaction of the incident electron wave with the three-dimensional crystal potential into successive scattering processes on thin crystal disks

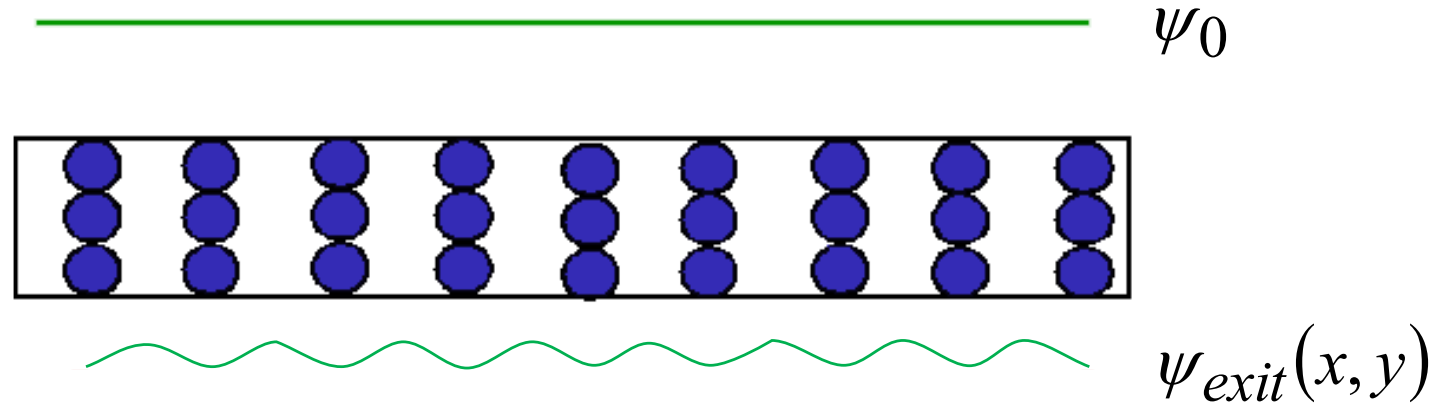


Schematic representation of the multislice method: A) "thick" sample, B) decomposition into thin slices, C) thin slice with phase lattice corresponding to projected crystal potential

Insert:

Approximation of the weak phase object (WPO)

invading
plane wave



- Outgoing wave $\psi_{exit}(x, y)$ is only modulated in phase with unchanged amplitude
- Wavelength shortening at the location of the atomic columns - electrons are accelerated by increased (positive) crystal potential → Bending of the wavefront
- simple approach only for
 - a) extremely thin crystalline objects of typically $< 1\text{nm}$ thickness (*much more complex wave functions for thicker crystalline samples due to dynamic electron diffraction*)
 - b) Amorphous objects consisting of light elements (e.g. biological objects) with a thickness of a few 10 nm

WPO Approximation (insertion)

$$|\psi_0| = 1, \text{ small phase shift } \varphi$$

$$\psi_{exit}(x, y) = |\psi_0| \exp(i\varphi(x, y)) \approx 1 + i\varphi(x, y) + \dots$$

- Phase shift φ for very thin samples proportional to the projected crystal potential

$$V_p(x, y)$$

- Absorption negligible



Transmission function for a weak phase object with $\varphi(x, y) = \sigma V_p(x, y)$

σ : Interaction constant (wavelength, electron charge and electron mass)

For very thin crystalline objects, the phase of the transmitted wave function is in good approximation linearly dependent on the projected internal potential of the sample

- Problem with imaging weak phase objects: no contrast

$$|\psi_{exit}(x, y)|^2 = |1 + i\varphi(x, y)|^2 \approx 1$$



phase of the object wave must also be shifted by $\pm \pi/2$ to achieve contrast
(see contrast transfer function)

6.2 High-resolution TEM: Dynamic electron diffraction and image formation

Multislice method

Calculation of the wave function in two steps for each slice:

1. Interaction of the electron wave with the two-dimensional projected Crystal potential

→ Mathematical description by phase lattice function

Thin disk behaves like a pure phase object

projected crystal potential $V_p(x, y) = \frac{1}{\Delta z} \int_z^{z+\Delta z} V(x, y, z) dz$

Phase shift of the electron wave proportional to V_p



Phase lattice function

$$q(x, y) = \exp(i\sigma V_p(x, y))$$

Interaction constant

$$\sigma = \frac{2\pi m e \lambda}{h^2}$$

2. Propagation of the electron wave in a vacuum via slice thickness Δz up to the next phase lattice function

→ Mathematical description by Fresnel propagator

6.2 Dynamic electron diffraction in the HRTEM

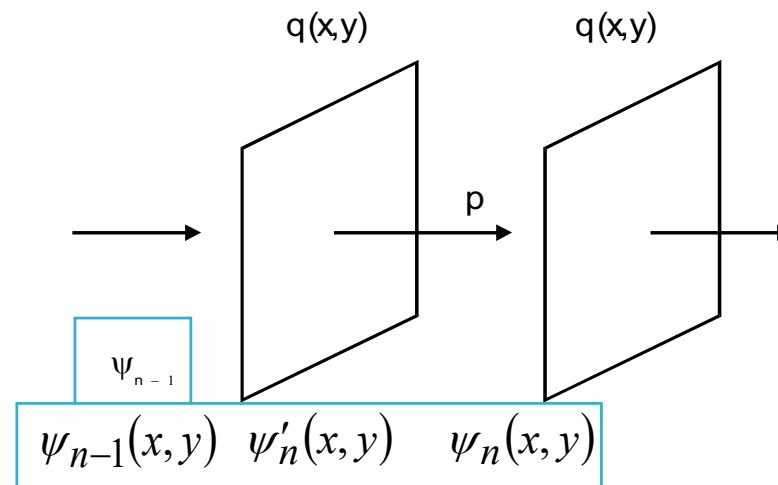
Multislice process

Wave function after propagation through the nth slice ψ_n

- Abrupt phase shift due to phase lattice function $q(x, y) = \exp(i\sigma V_p(x, y))$

$$\psi'_n(x, y) = \psi_{n-1}(x, y)q(x, y)$$

- Wave propagation in the disk with thickness Δz : Description by Fresnel propagator $p(x, y)$



p : Fresnel Propagator
 q : Phase lattice function

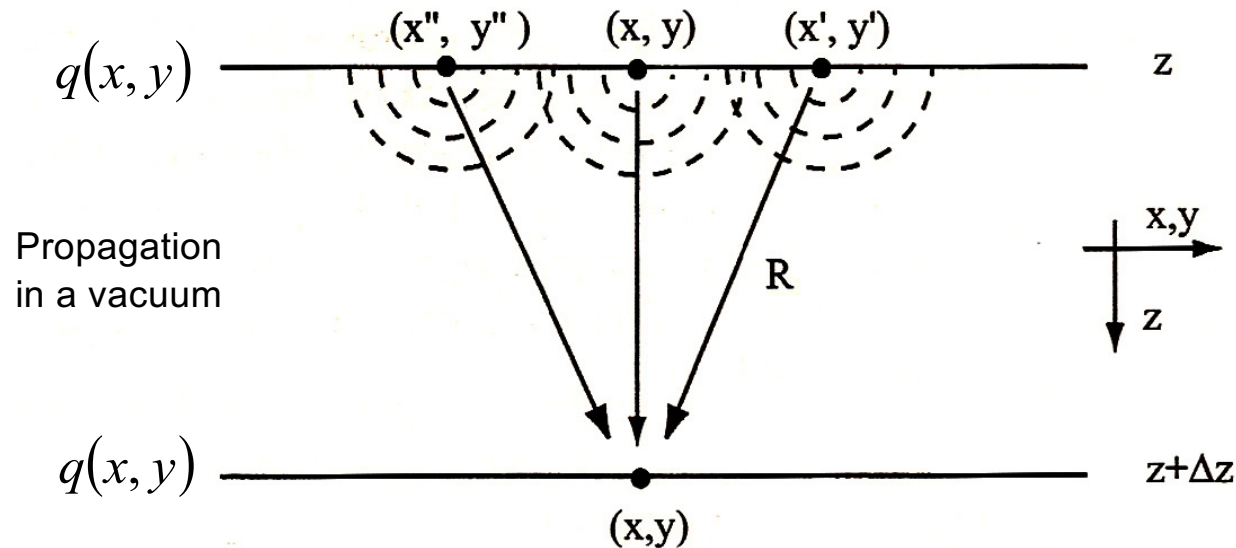
$$\psi_n(x, y) = \{ \psi_{n-1}(x, y)q(x, y) \} \otimes p(x, y)$$

6.2 Dynamic electron diffraction in the HRTEM

Multislice method: Propagation of the wave field

- Description of the propagation of the electron wave in a vacuum between the scattering planes of individual crystal disks by the Fresnel propagator $p(x,y)$
- The Fresnel propagator is based on the *Huygens-Fresnel principle*

 Each point of a wave front is again the starting point of a secondary spherical wave



- Physical interpretation of the Fresnel propagator:
Propagation of $\psi(x,y)$ in z to $z + \Delta z$
"Emission" of a spherical wave at every point (x,y) in z
Interference of the spherical waves at each point (x,y) in $z + \Delta z$

Kirkland, Advanced Computing in Electron Microscopy, Fig. 6.5


6.2 Dynamic electron diffraction in the HRTEM

Fresnel propagator

- Phase is constant along the wave on the radius Δz from the origin O'
- Along path AB , the wave travels an additional distance to the next phase lattice function

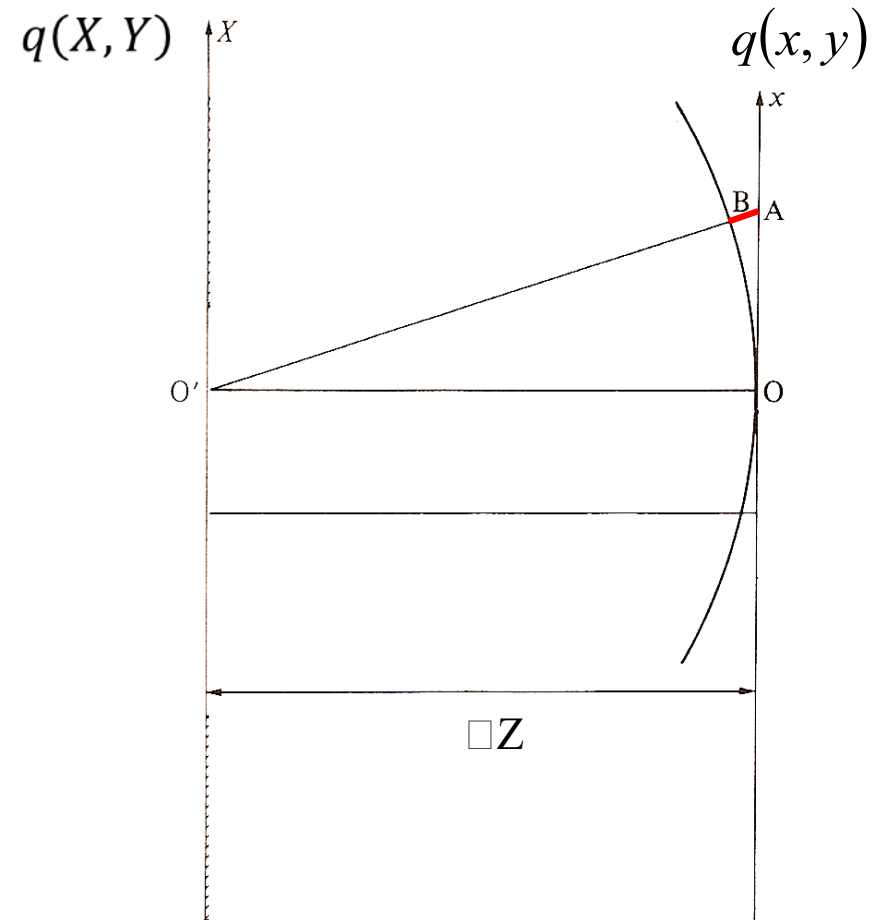
$$AB = \sqrt{\Delta z^2 + [x_A - X]^2} - \Delta z \approx \frac{[x_A - X]^2}{2\Delta z}$$

(approximation results from strong tendency to forward scattering - only significant contributions from waves with small angle)

 additional phase shift at point A compared to O,

Description by **phase factor P_A**

$$P_A = \exp\left(-2\pi i \frac{(x_A - X)^2}{2\Delta z \lambda}\right)$$



Spherical wave is emitted at a point O'

J. Spence, Experimental HRTEM, Fig. 3.2

6.2 Dynamic electron diffraction in the HRTEM


Fresnel propagator

- Fresnel propagator: Operator for describing the propagation of the wave field in two dimensions x, y with a slice thickness Δz

$$p(x, y) = 1/(i\lambda\Delta z) \exp\left(-\pi i \frac{(x^2 + y^2)}{\Delta z \lambda}\right)$$

- Wave function at the exit surface of a disk with the thickness Δz :
Coherent superposition of spherical waves in plane n with coordinates (x, y) emanating from all points ψ'_n of with coordinates (X, Y)

mathematical description through a convolution operation


$$\psi_n(x, y) = \int_{-\infty}^{\infty} \int_{-\infty}^{\infty} \psi'_n(x - \bar{x}, y - \bar{y}) p(\bar{x}, \bar{y}) d\bar{x} d\bar{y} = \psi'_n(x, y) \otimes p(x, y)$$


- Wave function at the n th disk:
Multiplication with the phase lattice function and convolution with the Fresnel propagator

$$\psi_n(x, y) = \{\psi_{n-1}(x, y)q(x, y)\} \otimes p(x, y)$$

Multislice formalism

- Exit wave function on the underside of the sample - **N-fold execution of the double operation: Scattering on the phase lattice/Fresnel propagation** (*simulation of the entire sample thickness with $t = N \cdot Dz$*)
- Application of the convolution theorem \rightarrow Replace the convolution operation in local space with a multiplication in reciprocal space (*shorter calculation time*)

- Convolution operation of the wave function with the Fresnel propagator


$$\psi_n(x, y) = \int_{-\infty}^{\infty} \int_{-\infty}^{\infty} \psi'_n(x - \bar{x}, y - \bar{y}) p(\bar{x}, \bar{y}) d\bar{x} d\bar{y} = \psi'_n(x, y) \otimes p(x, y)$$

- Convolution theorem $FT(\psi'_n(x, y) \otimes p(x, y)) = \psi'_n(u, v) p(u, v)$

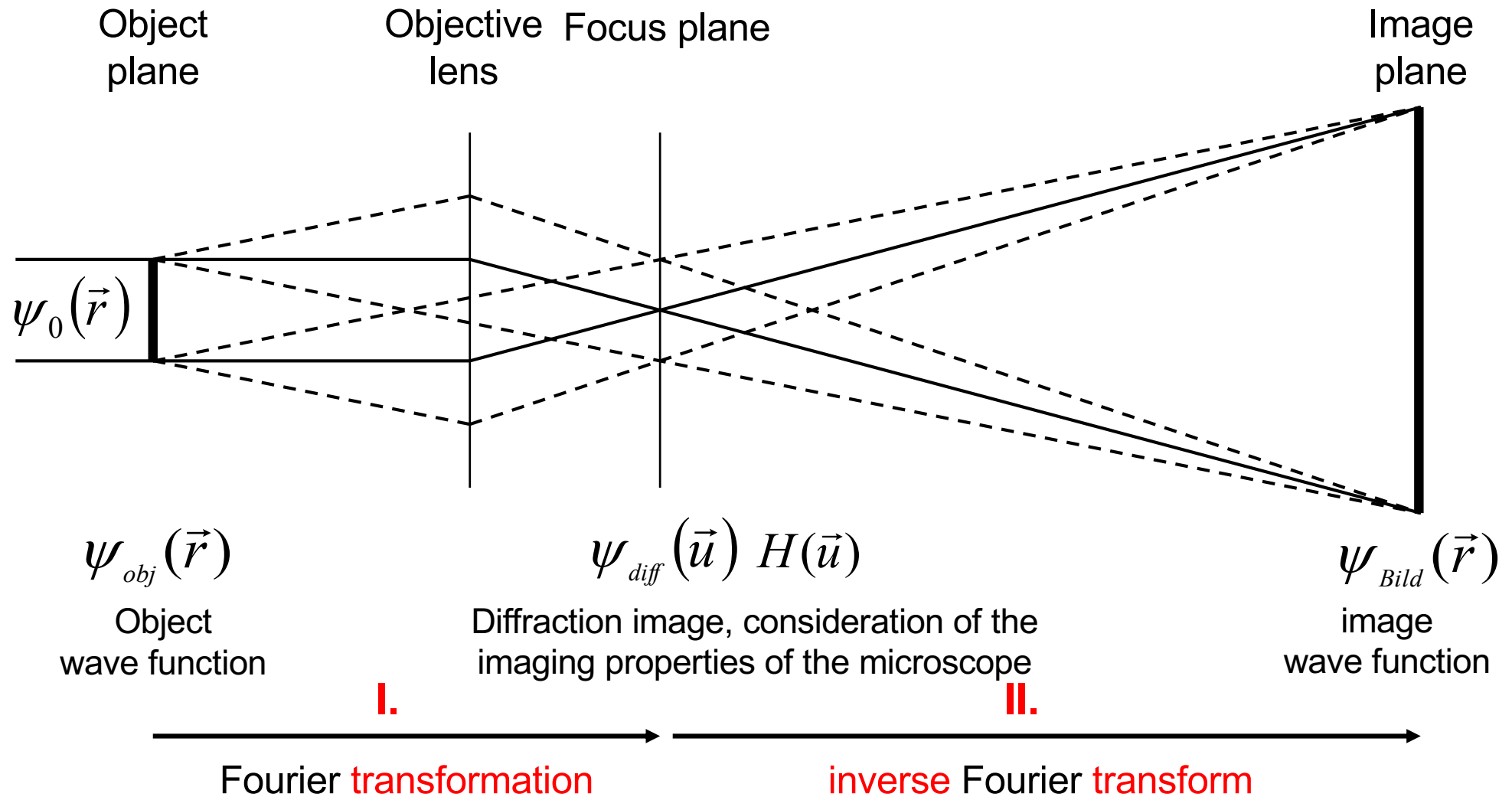
u,v: spatial frequencies

Fourier transform of the Fresnel propagator: $p(u, v)$

- **next step - imaging the wave function on the underside of the sample through the microscope**

6.3 Image formation in the HRTEM

Imaging process in the transmission electron microscope



Mathematical description of the mapping process

- I. Wave function in the plane of the diffraction pattern (Fourier decomposition)

$$\psi_{diff}(\vec{u}) = FT(\psi_{obj}(\vec{r}))$$

Change in the wave function due to lens aberration and partial coherence

$$\psi'_{diff}(\vec{u}) = \psi_{diff}(\vec{u})H(\vec{u}) \quad H(\vec{u}) \text{ Contrast transfer function}$$

- II. Wave function in the image plane (Fourier synthesis)

$$\psi_{Bild}(\vec{r}) = FT^{-1}(\psi'_{diff}(\vec{u})) = FT^{-1}(\psi_{diff}(\vec{u})H(\vec{u}))$$



Image intensity

$$I_{Bild} = \psi_{Bild}(\vec{r}) \cdot \psi_{Bild}^* = |\psi_{Bild}|^2$$

6.3 Image formation in the HRTEM

Contrast transfer function

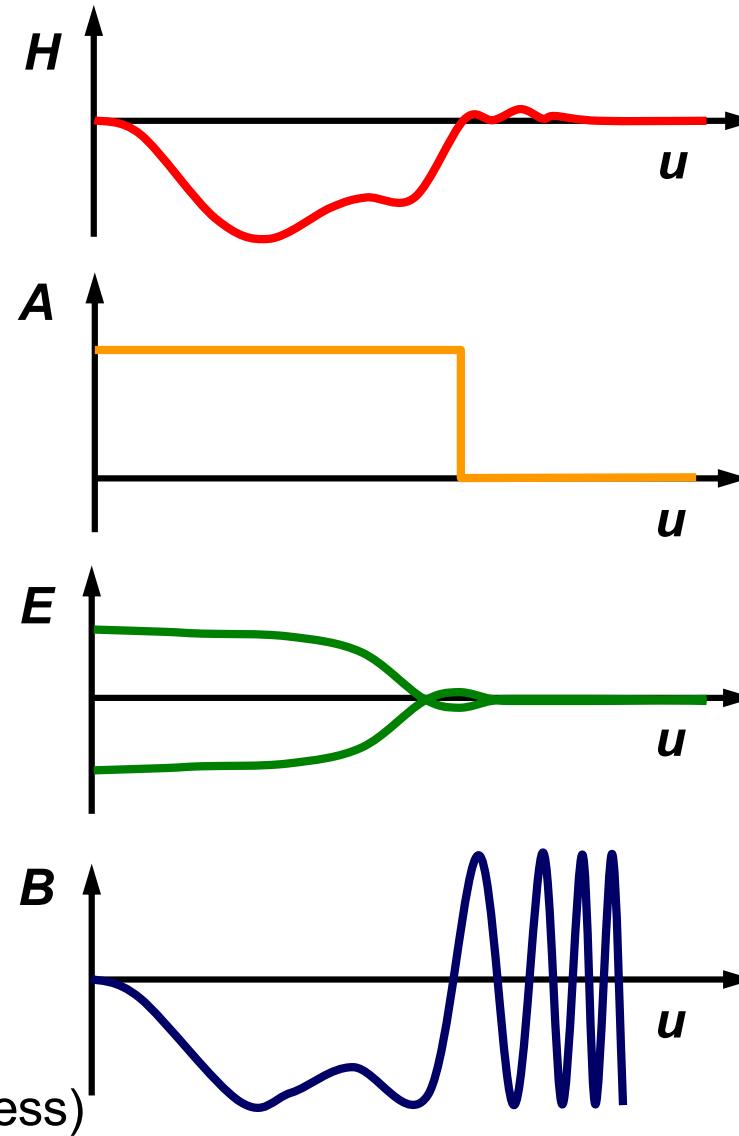
$$H(\vec{u}) = B(\vec{u})A(\vec{u})E(\vec{u})$$

In the simplest case, radial symmetry:
Space frequency u instead of \vec{u}

$A(u)$ - Aperture function

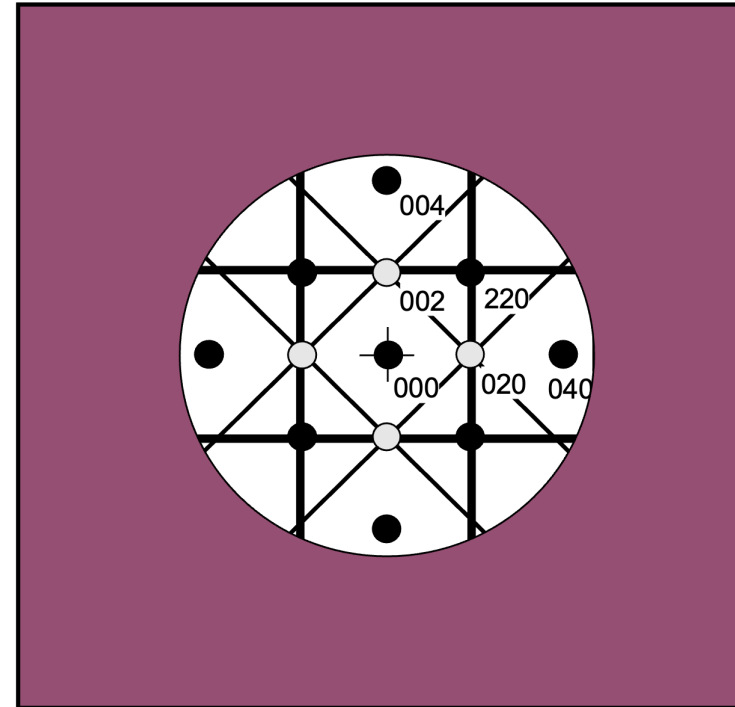
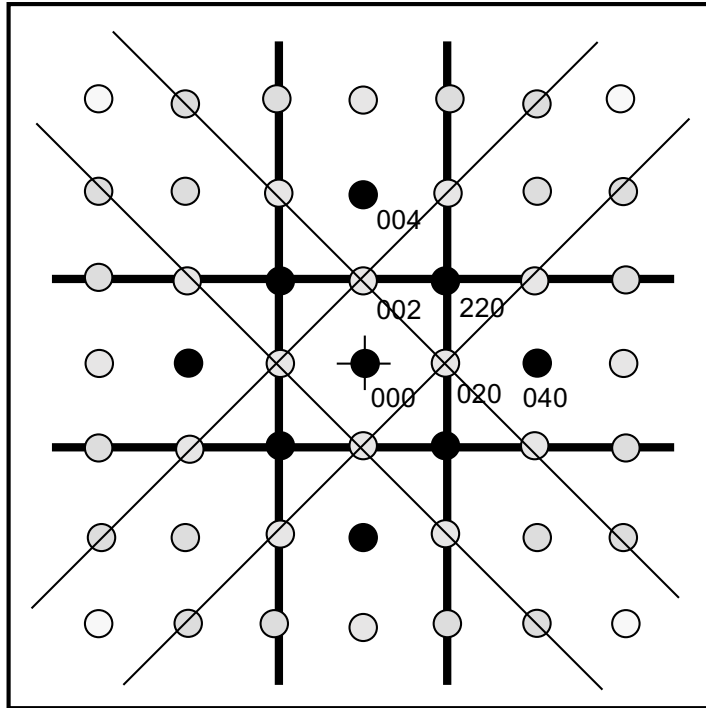
$E(u)$ - Envelope function
(damping function)

$B(u)$ - wave transfer function
(Phase shift
through mapping process)



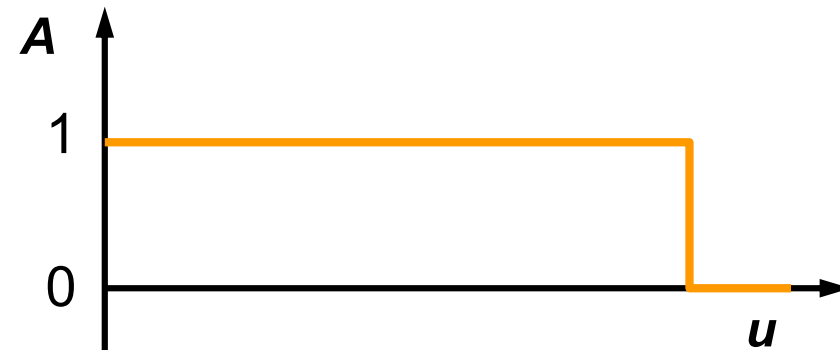
6.3 Image formation in the HRTEM

Aperture function $A(u)$



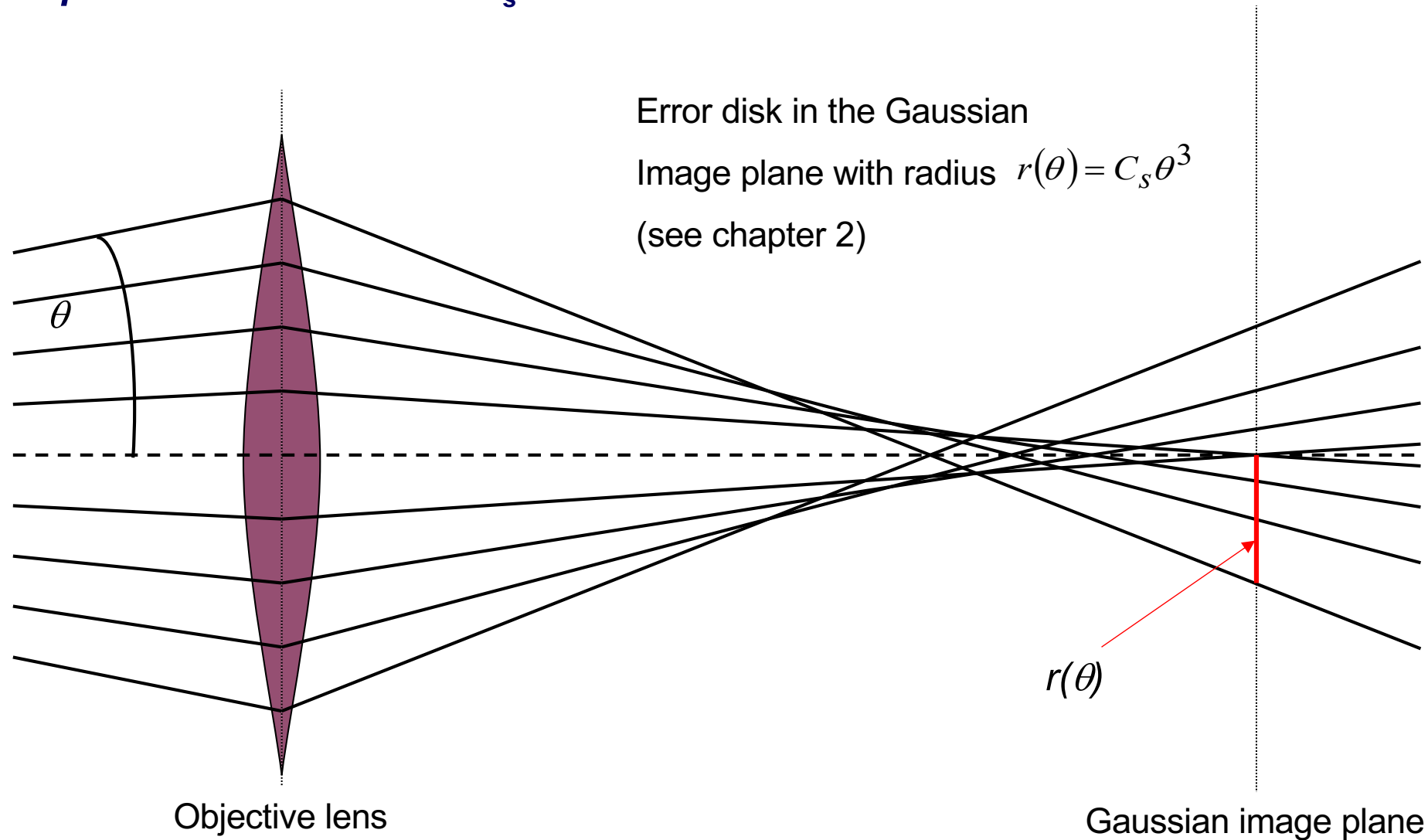
Schematic diffraction pattern
(left)

Effect of an aperture (right)



6.3 Image formation in the HRTEM

Wave transfer function $B(u)$: Effect of the aperture error with aperture error constant C_s



6.3 Image formation in the HRTEM

Objective lens end focus Δf

- "Sharp" image no longer has the same meaning in HRTEM as in geometric optics in terms of the lens equation

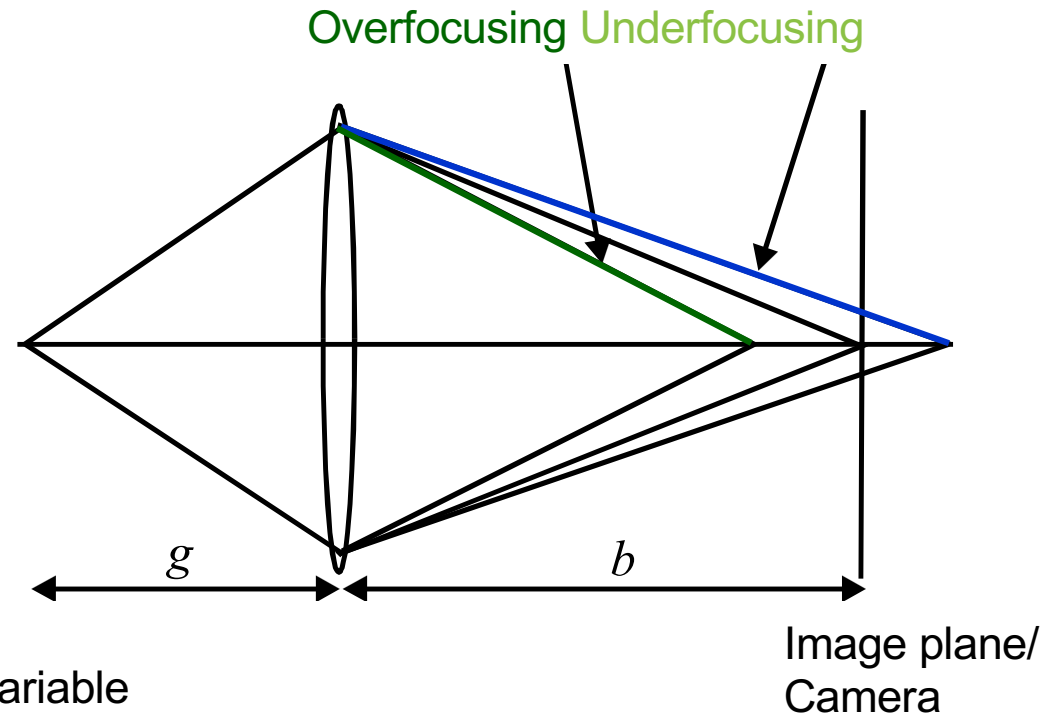
$$\frac{1}{f} = \frac{1}{g} + \frac{1}{b}$$

- Defocus Δf = deviation of the focal length from the focal length f , which results in a "sharp" image in geometric optics
- Focal lengths of magnetic lenses are variable

Underfocusing (extension of the focal length), "sharp" image behind the image plane $\Delta f < 0$

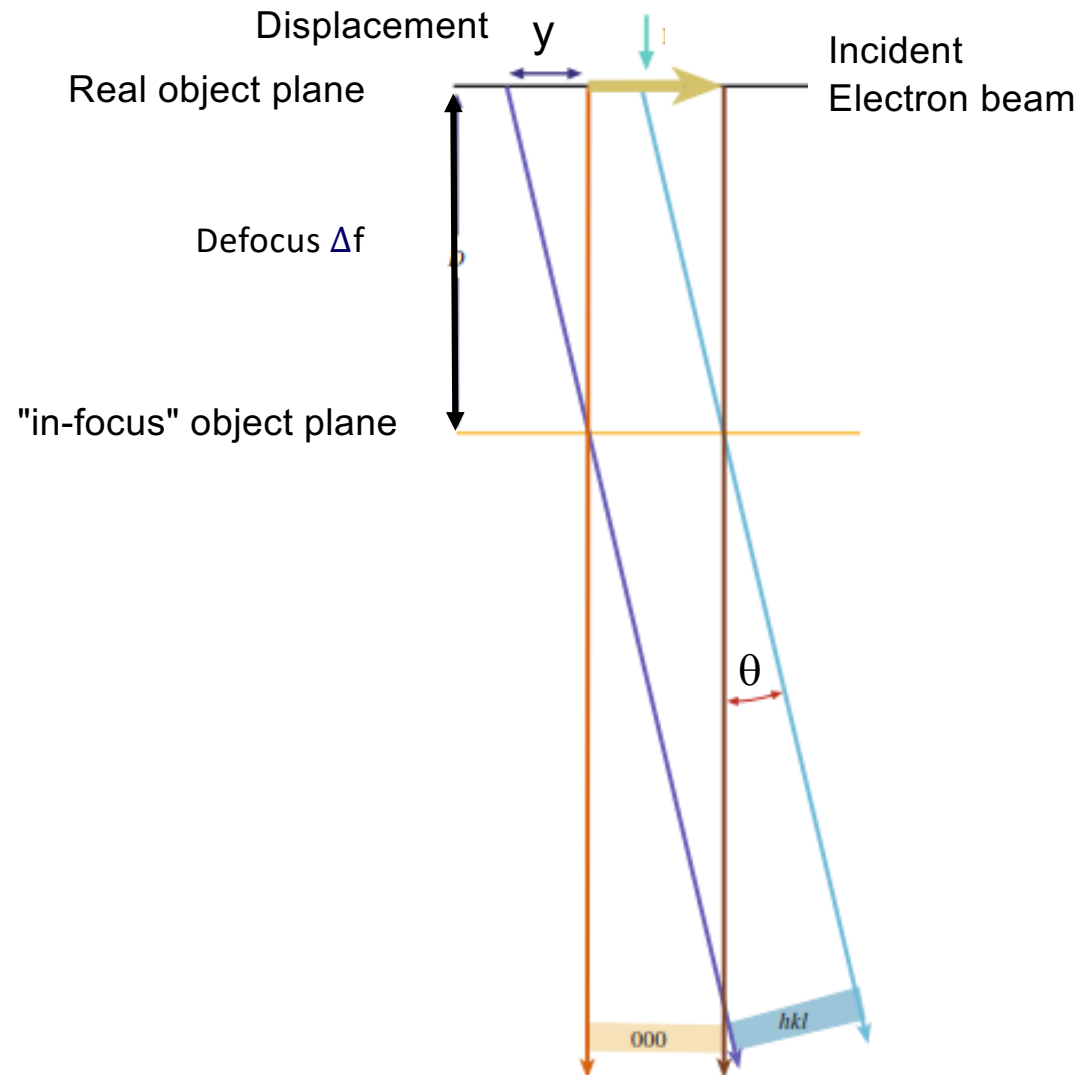


Overfocusing (shortening of the focal length), "sharp" image is in front of it $\Delta f > 0$
(Light optics: focal length fixed - defocusing only by changing the object distance)



6.3 Image formation in the HRTEM

Wave transfer function $B(u)$: Effect of defocus Δf



Displacement y as a function of θ
for small angles

$$y = \Delta f \theta$$

D.B. Williams, B.C. Carter, Transmission Electron Microscopy, Fig. 11.13

6.3 Image formation in the HRTEM

Total displacement $\delta(\theta)$ due to aperture error C_s and defocus $\Delta\phi$ for a certain value of θ

$$\delta(\theta) = C_s \theta^3 + \Delta f \theta$$

For an area of θ

$$D(\theta) = \int \delta(\theta) d\theta = \frac{C_s}{4} \theta^4 + \frac{\Delta f}{2} \theta^2$$

Phase shift $\chi(\theta)$ due to aperture error and defocus

$$\chi(\theta) = D(\theta) \frac{2\pi}{\lambda} = \frac{\pi}{2\lambda} C_s \theta^4 + \frac{\pi}{\lambda} \Delta f \theta^2$$

- Angle-dependent phase shift \rightarrow Strong "distortion" of the wave function
- Partial compensation of the phase shift by defocus $\Delta\phi$ (negative values of $\Delta\phi$)

6.3 Image formation in the HRTEM

- Typical values for C_s : 0.5 mm (very good lens), 3 mm (standard)
- More complex expression for χ if higher-order mapping errors have to be taken into account
- Higher order aberrations can depend on the azimuth angle in the diffraction plane

Conversion of angle θ into spatial frequency u , d_{hkl} : (lattice plane) distances in real space

$$2d_{hkl} \sin \theta_B \approx 2d_{hkl} \theta_B = n\lambda \Rightarrow 2\theta_B d_{hkl} = \lambda \Rightarrow 2\theta_B := \theta = \frac{\lambda}{d_{hkl}} = \lambda u$$

Small angles for n=1

$$\chi(u) = \frac{\pi}{2} C_s \lambda^3 u^4 + \pi \Delta f \lambda u^2$$

Wave transfer function

$$B(u) = \exp(-i\chi(u))$$

6.3 Image formation in the HRTEM

Contrast transfer for a weak phase object

$$B(u) = \exp(-i\chi(u)) = \cos \chi(u) - i \sin \chi(u)$$

here for presentation reasons

u : radial coordinate in the diffraction pattern

x, y : Cartesian coordinates in object- and image wave function

Only the imaginary part of $B(u)$ is relevant for a weak phase object

$$\psi_{obj}(x, y) = |\psi_0| \exp(i\varphi(x, y)) \approx 1 + i\varphi(x, y) + \dots$$

with $|\psi_0| = 1$

$$\psi'_{diff}(u) = \delta(0) + i\tilde{\varphi}(u) \exp(-i\chi(u))$$

$$\tilde{\varphi} = FT(\varphi)$$

$$\psi_{image}(x, y) = 1 + FT^{-1}\{i\tilde{\varphi}(u)(\cos\chi(u) + i \sin(u))\}$$

$$I = \psi_{image}(x, y) \cdot \psi_{image}^*(x, y) = 1 + 2FT^{-1}\{\tilde{\varphi}(u)\sin\chi(u)\} + \text{Higher terms}$$

~~Order in φ~~



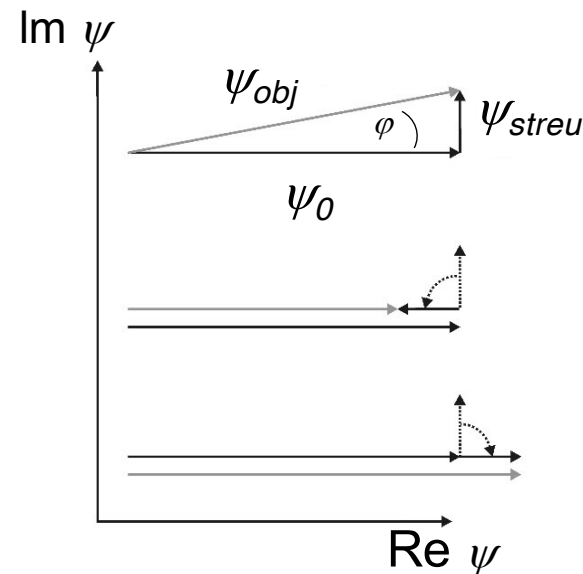
$\sin \chi(u)$ is referred to as the *phase contrast transfer function (PCTF)*

The PCTF describes the effect of the phase shift χ of defocus and C_s on the image wave function of a weak phase object

The optimum phase shift for a weak phase object is ± 90 degrees with $\sin\chi = \pm 1$

6.3 Image formation in the HRTEM


Optimal phase contrast transfer for a weak phase object



For small angles φ

$$\psi_{obj}(x, y) = |\psi_0| \exp(i\varphi(x, y)) \approx 1 + i\varphi(x, y) + \dots$$

$|\psi_{obj}|^2 = |\psi_0|^2$  Object shows no contrast in the TEM image with *aberration-free* lenses

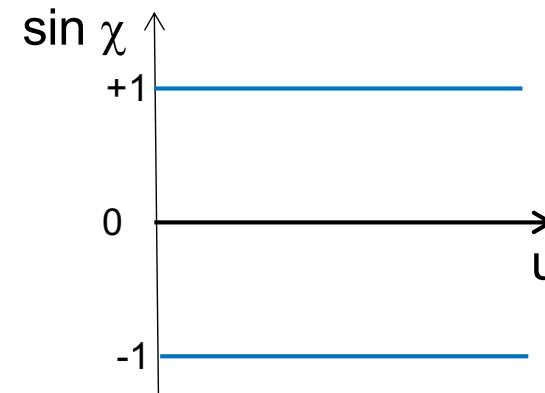
Additional phase shift by ± 90 degrees  best phase contrast with $\sin\chi = \pm 1$

6.3 Image formation in the HRTEM

Ideal PCTF for a weak phase object

$$\sin \chi = -1 \text{ or } \sin \chi = 1$$

over a maximum range of spatial frequencies u

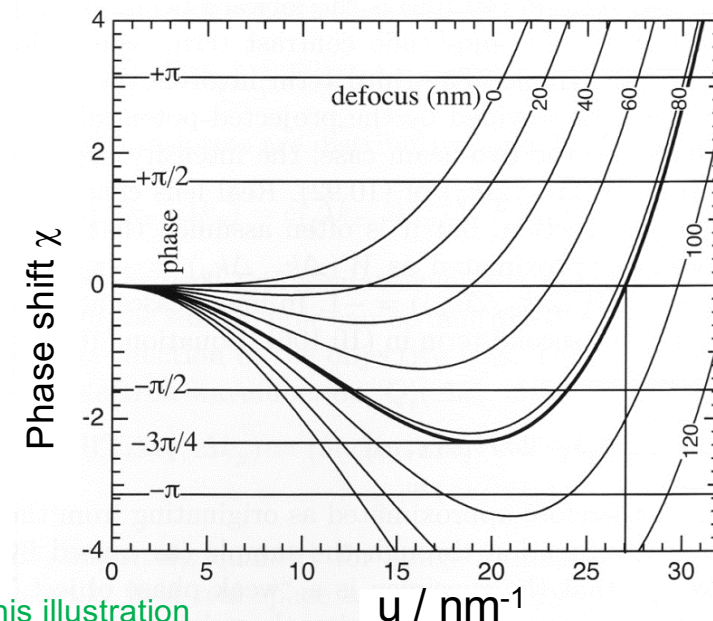


What does the optimum *real* PCTF look like? A matter of definition!

For a weak phase object: e.g. maximum range of spatial frequencies u that are transmitted with a phase shift χ between -60° and -120°

$$\chi(u) = \frac{\pi}{2} \lambda^3 C_s u^4 + \pi \lambda \Delta f u^2$$

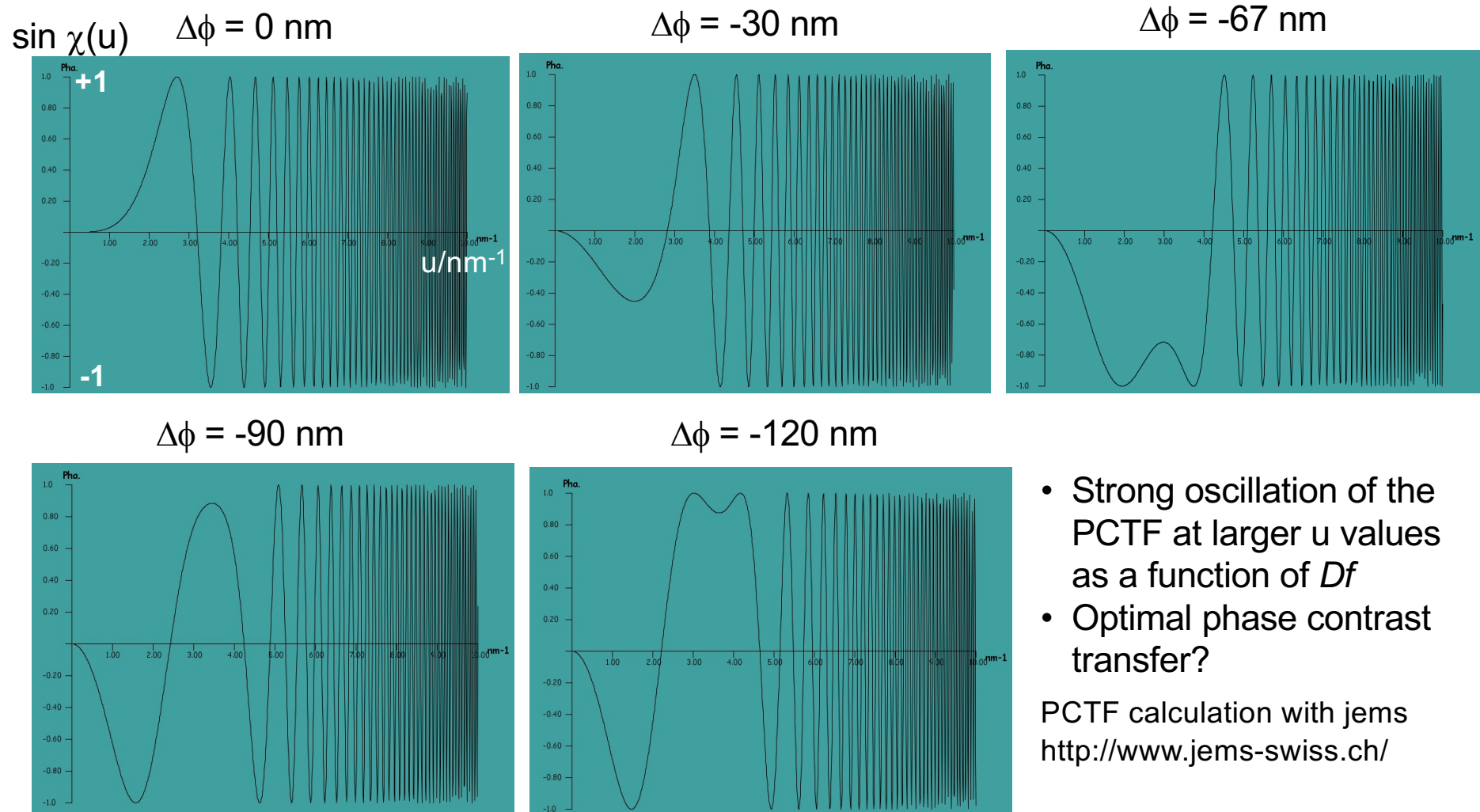
For a microscope with
 $c_s = 2.3 \text{ mm}$
 300 keV
 $\lambda = 1.97 \text{ pm}$



B. Fulz, J.M. Howe, Transmission electron microscopy and diffractometry of materials, Fig. 10.15, **note: negative sign is missing for underfocus in this illustration**

6.3 Image formation in the HRTEM

PCTF for Philips CM200 FEG/ST microscope with $C_s = 1.2 \text{ mm}$, 200 keV and various $\Delta\phi$ values: $\sin \chi(u)$ plotted as a function of u / nm^{-1}



6.3 Image formation in the HRTEM

- Definition: Scherzer defocus Δf_{Sch} (optimal defocus) when

$$\frac{d\chi}{du} = 0 \quad \chi_{min} = -\frac{3\pi}{4}$$

$$\Delta f_{Sch} = -1,15\sqrt{C_S\lambda}$$

Pre-factor varies in the literature, e.g. 1.2 instead of 1.15

- First zero crossing of the PCTF
- Definition of Scherzer resolution is the reciprocal value of u_{Sch}

$$u_{Sch} = 1,51 \cdot C_S^{-1/4} \cdot \lambda^{-3/4}$$

$$r_{Sch} = 0,66 \cdot C_S^{1/4} \cdot \lambda^{3/4}$$

- Example: $E_0 = 200$ keV, $\lambda = 2.5079 \cdot 10^{-12}$ m, $C_S = 1.2$ mm
Philips CM200 FEG/ST

$$\Delta f_{Sch} = -63 \text{ nm}$$

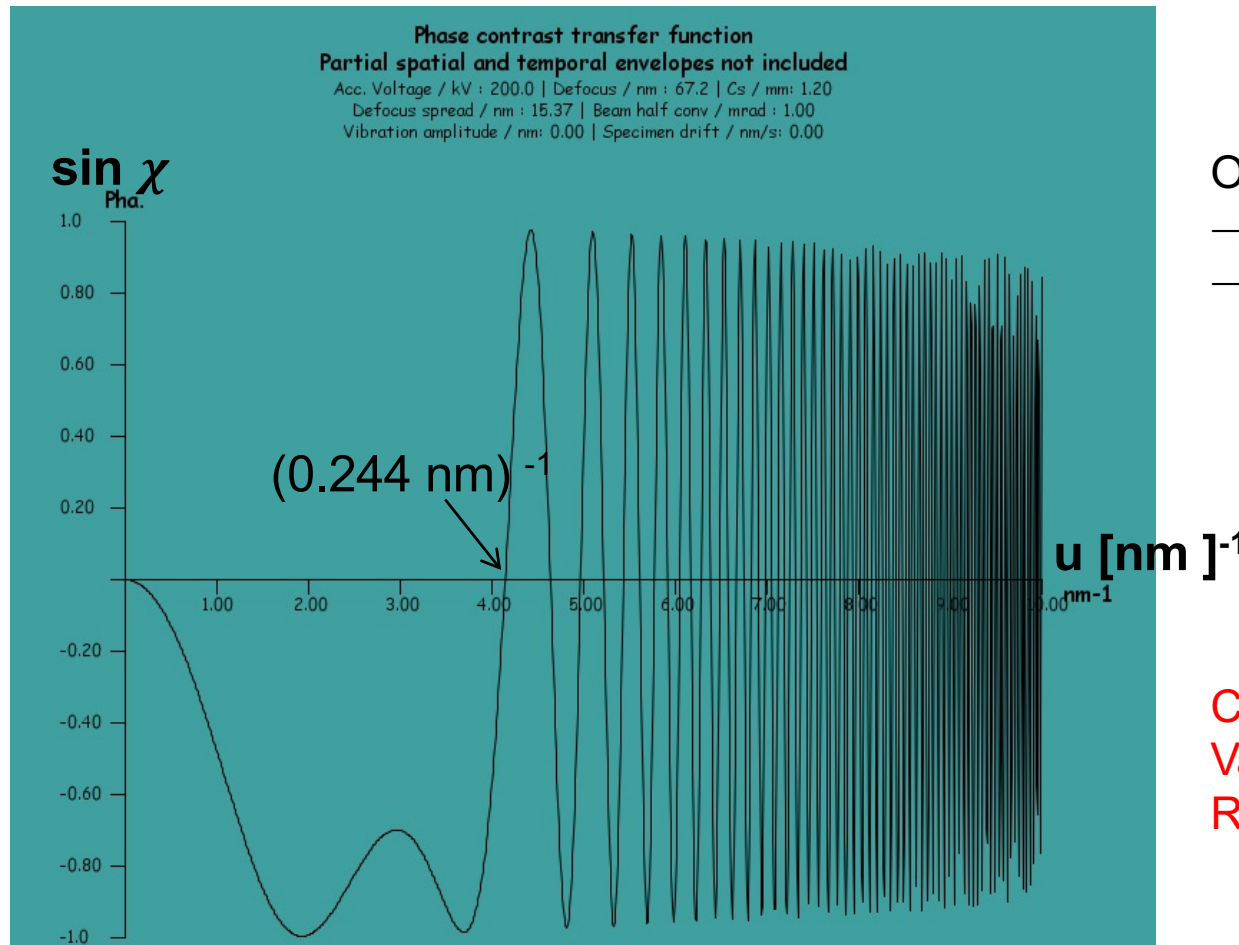
$$r_{Sch} = 2,44 \cdot 10^{-10} \text{ m} = 0,244 \text{ nm}$$

- Optimal defocus also depends significantly on the spatial frequency spectrum of the object

6.3 Image formation in the HRTEM

PCTF for Philips CM200 FEG/ST: $E_0 = 200 \text{ keV}$, $\lambda = 2.5079 \cdot 10^{-12} \text{ m}$,

$$C_S = 1.2 \text{ mm}, Df_{\text{Sch}} = -67$$



Oscillating behavior of the PCTF
→ Phase shift depending on u
→ "Distortion" of the wave function

Contrast transfer at high
Values of u ?
Resolution better than 1 \AA ?

PCTF calculation with jems
<http://www.jems-swiss.ch/>

6.3 Image formation in the HRTEM

Envelope $E(u)$: Damping of the transfer of large spatial frequencies by partial spatial and temporal coherence

$$H(\vec{u}) = B(\vec{u})A(\vec{u})E(\vec{u})$$

Cause of partial spatial coherence:

not a perfectly flat incident wave, but curvature of the wave front due to the convergence angle of the incident wave's ray bundle

Parameters: Convergence half-angle with typical values between 0.5 and 2 mrad


Cause of partial temporal coherence:

Instabilities of the high voltage and lens currents, energy distribution of the electrons in combination with chromatic aberration (chromatic aberration constant C_c)

Parameters: Defocus scattering Δ

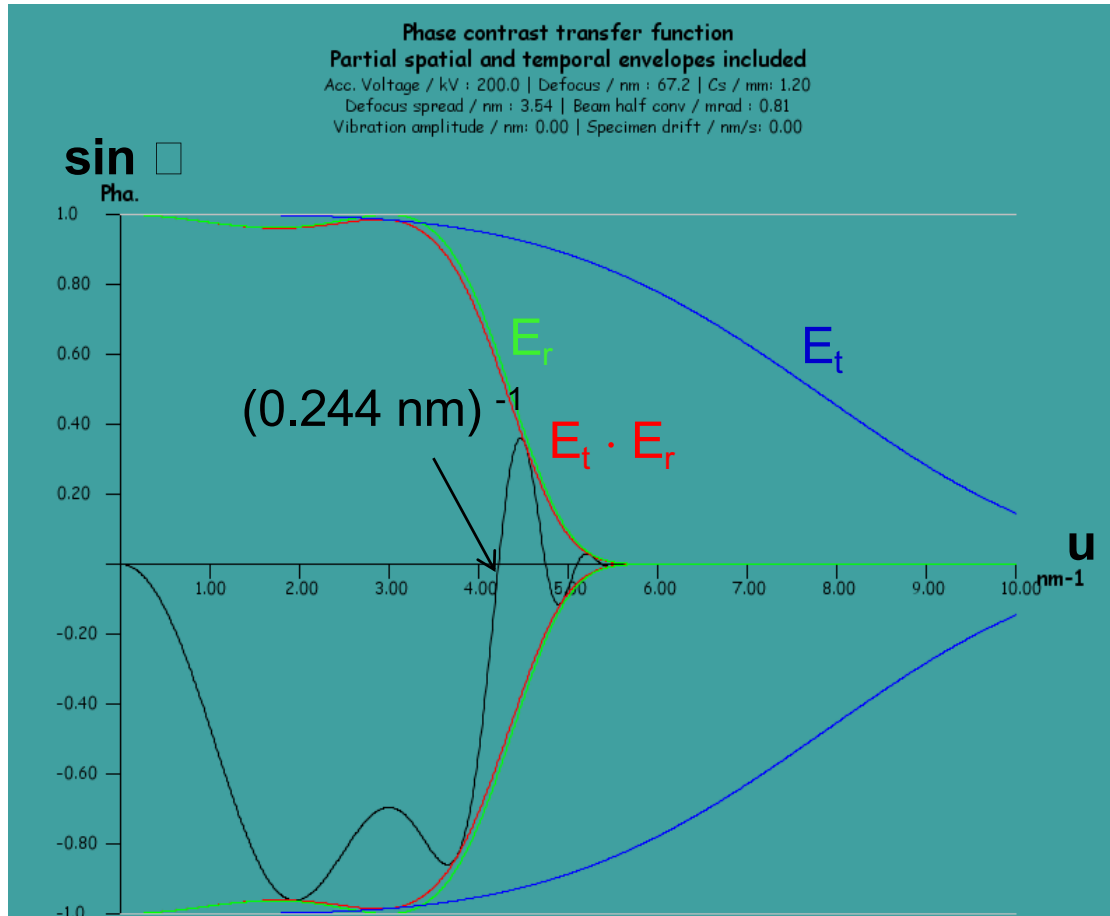
$$\Delta = C_c \sqrt{\frac{(2\Delta I)^2}{I^2} + \frac{\Delta U^2}{U^2} + \frac{\Delta E^2}{E^2}}$$

Typical values: $\Delta I/I = 10^{-6}$, $DU/U = 10^{-6}$, $DE = 1$ eV
For Philips CM200: $E = 200$ keV, $C_c = 1.2$ mm

 $\Delta = 6.5$ nm

6.3 Image formation in the HRTEM

PCTF for Philips CM200 FEG/ST: $E_0 = 200 \text{ keV}$, $\lambda = 2.5 \cdot 10^{-12} \text{ m}$, $C_S = 1.2 \text{ mm}$



$$\Delta f_{\text{Sch}} = -67 \text{ nm}$$

$$\Delta = 6.5 \text{ nm}$$

Convergence half angle 1 mrad

E_t : Enveloppe for partial temporal Coherence

E_r : Enveloppe for partial spatial Coherence

$u \text{ [nm]}^{-1}$

Calculation of the envelope see further literature, e.g.

B. Fulz, J.M. Howe, "Transmission electron microscopy and diffractometry of materials", chap. 10

or

D.B. Williams, C.B. Williams, "Transmission Electron Microscopy", Chapter 28

PCTF calculation with jems
<http://www.jems-swiss.ch/>

- High-resolution (HR)-TEM images are interference contrast images from which the exact position of atomic columns cannot be determined intuitively.
- The most important parameters for HRTEM imaging are the sample thickness, the defocus and the properties of the microscope, which determine the partial spatial and temporal coherence of the electrons.
- HRTEM image simulations are essential for a detailed understanding of HRTEM images.
- The exit wave function at the bottom of the sample (object wave) must be calculated by applying dynamic diffraction theory (Bethe Bloch wave method or multislice method).
- As with all imaging systems with lenses, the image is described by the Fourier transformation of the object wave (wave function in the diffraction plane) and subsequent inverse Fourier transformation (wave function in the image wave).
- The imaging properties of the microscope are described by the contrast transfer function $H(u)$, which describes the influences of the objective aperture $A(u)$, lens aberrations and defocus (spatial frequency-dependent phase shift $B(u)$) as well as the attenuation of large spatial frequencies by partial spatial and temporal coherence $E(u)$.

- The *phase contrast transfer function* (PCTF) describes the transfer of spatial frequencies for a weak phase object. The PCTF is often used to characterize the resolution of the microscope.
- The best "point resolution" is achieved when the Scherzer defocus is set to transmit a maximum spatial frequency interval with phase shifts between 60 and 120 degrees.
- The best defocus for imaging an object is not necessarily the Scherzer defocus, but depends on the spatial frequency spectrum of the object.
- Today, high-resolution microscopes are often equipped with an aperture error corrector, which improves the resolution down to values of 0.05 nm. In this case, resolution is limited by partial temporal coherence (not shown in the lecture).